

Segmentation and Merging of Autonomous At-the-Limit Maneuvers for Ground Vehicles

Pavel Anistratov, Björn Olofsson, & Lars Nielsen

Division of Vehicular Systems, Department of Electrical Engineering

Linköping University, Sweden

E-mail: pavel.anistratov@liu.se

Topic: Vehicle Automation and Connection

To decrease the complexity of motion-planning optimizations, a segmentation and merging strategy for maneuvers is proposed. Maneuvers that are at-the-limit of tire friction are of special interest, since they appear in many critical situations. The segmentation points are used to set constraints for several smaller optimization problems for parts of the full maneuver, which later are merged and compared with optimizations of the full maneuver. The technique is illustrated for a double lane-change maneuver and for a 90°-turn maneuver. The results are obtained for the case when the desired splitting points are directly available from a database and when a linear interpolation of available splitting points is used. The resulting segmented and merged paths are close to optimal, with other state variables showing good match with the optimal solutions in general.

1 INTRODUCTION

Self-driving cars recently got a lot of attention, as well as other technologies that are used by them. Several competitions were held to promote driverless vehicle technology, notable examples are DARPA Grand Challenge and DARPA Urban Challenge, as well as events by private companies, of which one is the autonomous drive of the Bertha-Benz historic route [1]. With the development of new sensors, improved situation awareness, and increased available computation power, the cars could be made safer and more reliable, for example by making optimal decisions and maneuvers in case of a potentially dangerous situation [2]. One step to achieve this is to use online motion planners with realistic vehicle dynamic models [3]. A long planning horizon and a high re-planning frequency usually give a safer operation of the vehicle. However, with the increase of the planning horizon, the complexity of the motion-planning problem grows rapidly [4]. To decrease complexity, we are interested to split the full motion-planning problem into several segments, which are easier to solve, but still with close to optimal overall behavior. The research is in this paper illustrated with two example scenarios—a double lane-change maneuver, which is inspired by the double lane-change test (ISO 3888-2:2011), and a 90°-turn maneuver.

Using the optimization formulation for motion planning of the double lane-change maneuver from [5], the optimal trajectories were obtained for varying parameters of the problem: initial velocity, distance to the obstacle, and length and width of the obstacle. With a modification of the formulation in [5], trajectories for the 90°-turn maneuver were obtained by varying initial velocity as well as entry and exit distances of the turn. By analyzing the obtained trajectories, it was noticed that there are several points that split the trajectories by different behavior. These segmentation points are used to perform optimizations for smaller parts of the full problem, to later combine them into the trajectory of the full considered maneuver.

2 MODELING AND OPTIMIZATION

The models and parameters for a passenger vehicle are adopted from [6], where the model is referred to as ST WF. The model includes a single-track (ST) model for the chassis, the Pacejka Magic Formula [7] with weighting functions (WF) to com-

pute the tire forces [7], and a first-order system for the wheel dynamics. The vehicle and tire dynamics are formulated as $\dot{G}(\dot{\mathbf{x}}, \mathbf{x}, \mathbf{u}) = 0$ and $h(\mathbf{x}, \mathbf{u}) = 0$ for the states \mathbf{x} and inputs \mathbf{u} . The front wheel braking torque, T_f , the rear wheel driving/braking torque, T_r , and the steering angle, δ , are considered as the inputs with bounding constraints for the variable and the first derivative for all input variables.

The models were implemented using the Modelica language [8], and numerical optimizations were performed using the JModelica.org platform [9] and Ipopt software package for nonlinear optimization [10] together with the MA57 linear solver [11].

2.1 LDP for Double Lane-Change Maneuver

For the double lane-change maneuver (DLM), the track constraints for the full optimizations are formulated as in [5], with a smooth approximation of the Heaviside step function, which is also known as the logistic function. The optimization objective is to minimize the lane deviation penalty (LDP) [5].

2.2 LDP for Turn Maneuver

For the turn maneuver (TM), the LDP formulation from [5] is modified to fit a 90°-turn maneuver. Using the same smooth approximation of the Heaviside step function as in [5]:

$$\tilde{H}_{a_o}^{a_r}(a) = \frac{1}{2} + \frac{1}{2} \tanh\left(\frac{\pi}{a_r}(a - a_o)\right),$$

where a_o is the offset parameter and a_r is the rising distance parameter, we define the penalty function for the turn maneuver as:

$$\mathcal{P}(X(t), Y(t)) = 1 - \tilde{H}_{p_o}^{p_e}\left(\left(\frac{X(t)}{p_a}\right)^{p_e} + \left(\frac{Y(t)}{p_b}\right)^{p_e}\right). \quad (1)$$

The function is formulated with the help of parameters p_o , p_r , p_a , p_b , and p_e , such that values of $X(t)$ and $Y(t)$ outside of the superellipse (green lines in Figure 6) corresponding to the own lane give a decrease in the penalty and values inside the superellipse corresponding to the opposing lane give an increase in the penalty.

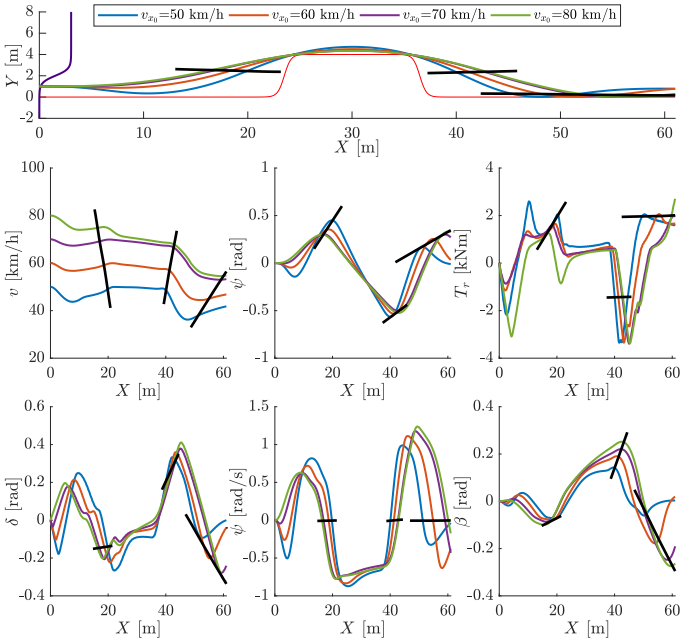


Figure 1: Splitting points for DLM.

The objective function for turn maneuvers is to minimize the following integral of the penalty function (1):

$$\int_0^{t_f} \mathcal{P}(X(t), Y(t)) dt,$$

where t_f is the total time of the maneuver, which is unknown *a priori*.

Another modification compared to DLM is the way maneuvers are visualized. For the DLM, the selected state variables are plotted against the longitudinal coordinate X , as in Figure 1. For the turn maneuver, most of the selected state variables are plotted against a phase variable Φ that is defined as:

$$\Phi = \arctan\left(\frac{Y}{X}\right).$$

3 SPLITTING METHOD: DESCRIPTION

The method to identify splitting points is derived from analysis of maneuvers for varying parameters defining the problem. This section describes general observations in this regard and gives two examples of splitting points for the double lane-change scenario and for the 90°-turn scenario.

3.1 Splitting Points

The splitting points are selected such that the original motion-planning problem can be divided into several segments, which are smaller and easier to find optimal solutions to. From the analysis of multiple motion-planning optimizations for varying parameters, it was noted that potential candidates for splitting points are extrema points of the vehicle orientation and yaw rate. Between these points, it is possible to compute a maneuver from a smaller optimization problem that is close to the corresponding part of the maneuver when the full optimization problem is considered. Only final constraints on a small subset of the state variables are needed to get a matching solution.

The potential splitting points for DLM and TM are illustrated in Figures 1 and 2 by black lines fitted to the obtained splitting points. The plots show optimal trajectories for the corresponding LDP formulation.

Figure 1 shows the paths and selected vehicle variables of DLM computed for different initial velocities v_0 (km/h). The splitting points are obtained as extrema of the vehicle orientation ψ . The splitting points correspond to zero value of the yaw

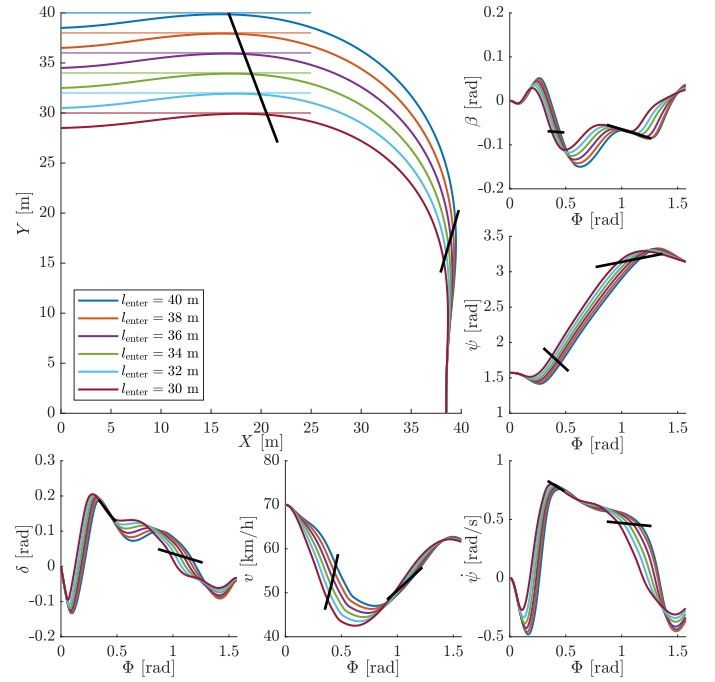


Figure 2: Splitting points for TM.

rate $\dot{\psi}$. They divide velocity profiles into three segments with different dominating behavior, which are also between extrema of the body-slip angle β . The vehicle position along the Y -axis is almost equal for all splitting points in the respective group.

The potential splitting points for TM are shown in Figure 2 based on optimal trajectories (shown in thick lines) found for the modified LDP formulation with varying entrance distance l_{enter} (m). Each thin line shows a part of the outer road boundary for the path of the corresponding color. For this maneuver, selection of splitting points at extrema of the vehicle orientation gives the middle segment that is much bigger than the other segments. A better splitting strategy corresponds to extrema of the vehicle yaw rate, where the first extremum is skipped, and the second splitting points are selected for the inflection point as illustrated in Figure 2. The black lines are fitted to the splitting points of the state variables. The shown state variables exhibit an appealing property of being equidistantly distributed along these lines.

The proposed segmentation points are used to divide the optimization of the full maneuver into several smaller parts, in a way that it is possible to compute a maneuver for the complete scenario by combining results from segmented optimizations.

3.2 Start and Final Constraints

The initial state of the optimization for each segment is fixed for the set of variables

$$\mathcal{S}_1 = \mathcal{S}_{1,e} \cup \mathcal{S}_{1,s}.$$

The set is formed by the union of the variables in $\mathcal{S}_{1,e}$, which are initialized to exact values and the variables in $\mathcal{S}_{1,s}$, which are constrained by predefined slack values. The first set

$$\mathcal{S}_{1,e} = \{X, Y, \psi, \dot{\psi}, v_x, v_y, \omega_f, \omega_r\}$$

includes the vehicle position, orientation, and yaw rate, all variables are in the global frame, velocities in the local frame, and angular velocities for the front and the rear wheel, respectively. The second set is

$$\mathcal{S}_{1,s} = \{\delta, \alpha_f, \alpha_r, T_f, T_r\},$$

where α_f and α_r are the tire-slip angles for the front and the rear wheel, respectively.

For the first segment, the initial values are considered to be known (e.g., the estimate of the current vehicle state). In this re-

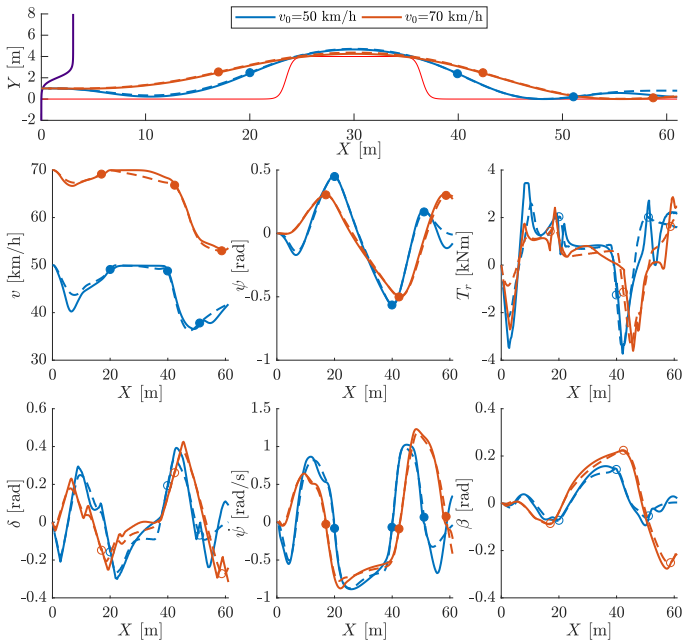


Figure 3: Reconstruction for DLM LDP.

search, they are chosen as in the optimization of the full maneuver. For the following segments, the initial values are set from the final values of the previous segmented optimization.

In addition to the final constraints on the vehicle position and orientation, as in the optimization of the full maneuver, there are additional constraints on the final vehicle velocity and yaw rate. These variables give the set of constrained variables for the final state (imposed with some slack value)

$$\mathcal{S}_2 = \{X, Y, \psi, \dot{\psi}, v_x, v_y\}. \quad (2)$$

3.3 What are Good Splitting Points?

Good splitting points allow dividing a full motion-planning problem into several smaller problems. Only a small number of the final constraints for each segment are needed to make the combined maneuver from segmented optimizations to be very similar to the maneuver obtained from the full optimization. Introduction of certain additional constraints for the segmented optimizations compared to the full optimization allows to remove some inequality constraints, *e.g.*, the road constraints. The objective function could thereby be left unchanged for each segment.

4 RESULTS

The proposed method is evaluated for DLM and TM. The method is first applied for maneuvers, where the splitting points are assumed to be known from a database. Then, the method is applied to compute a maneuver for splitting points not present in the database using an interpolation technique.

4.1 Trajectory Reconstruction

In this part, trajectories are reconstructed from splitting points, which are known from a database for the same maneuvers. The target values for the final variables are obtained from the values at the proposed splitting points in the trajectories of the optimization of the full maneuver with the same initial velocity, to see the best possible performance of the method.

Figures 3–4 and 6–7 show the comparison of the paths and selected vehicle variables from the segmented maneuver optimizations (shown in solid lines) and the optimization of the corresponding full maneuver (shown in dashed lines). The latter results were used to obtain information about the splitting points. The colored circles of the respective color show the variable values at the splitting points. The non-filled circles are used for vari-

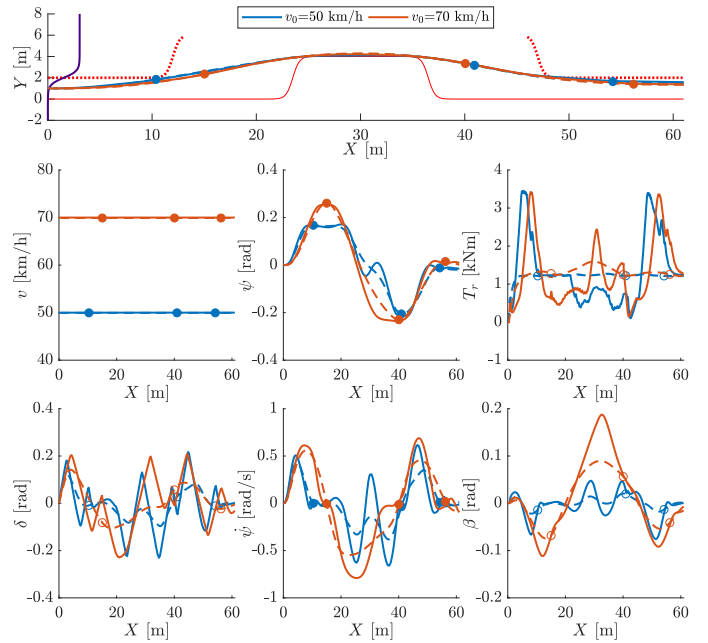


Figure 4: Reconstruction for DLM MT. The additional road boundary of the MT formulation is shown as the red dotted line.

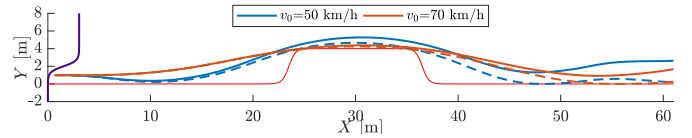


Figure 5: Simulation results for the reconstructed paths for DLM MT.

ables which have no final constraints in the segmented optimizations and the filled circles are used for the variables that have the final constraints, *i.e.*, they are part of the set \mathcal{S}_2 , see (2).

Figures 3–4 show the method applied to DLM, where information about splitting points is obtained from optimization of the full DLM for different initial velocities v_0 (km/h).

In general, the merged trajectories are very similar to the full trajectories in terms of the vehicle path, orientation, yaw rate, and steering angle. For the LDP formulation of DLM, the velocity deviates for the segmented optimization during the first segment and the last segment, the deviation is smaller for the high velocity (70 km/h) and larger for the low velocity (50 km/h). This is also visible for the rear wheel torque (T_r) in these segments.

In the first two rows of Table 1, the LDP objective function is computed for trajectories obtained by the optimization of the full maneuver and for the merged trajectories obtained by the segmented optimizations. The results are similar, as desired. However, the latter values are sometimes even smaller than the former since the optimization solver takes advantage of the allowed state discontinuities for a subset of the variables between the segments. The last row of Table 1 shows calculated values of the objective function for trajectories, which were obtained by simulating the vehicle model with merged optimal model inputs of the segmented optimizations (δ, T_f, T_r). Some values differ noticeably and these differences are related to the simulated trajectories. Figure 5 shows a comparison of selected simulated paths (solid lines) and optimized paths (dashed lines). The simulated path for initial velocity $v_0 = 50$ km/h deviates from the

Table 1: Computed LDP objective function values [m · s] for different initial velocities and problem formulations.

Name \ v_0 [km/h]	50	60	70	80
Opt., full maneuver	1.71	1.66	1.62	1.60
Opt., merged maneuver	1.63	1.61	1.58	1.62
Sim., merged maneuver	2.69	1.96	1.72	2.51

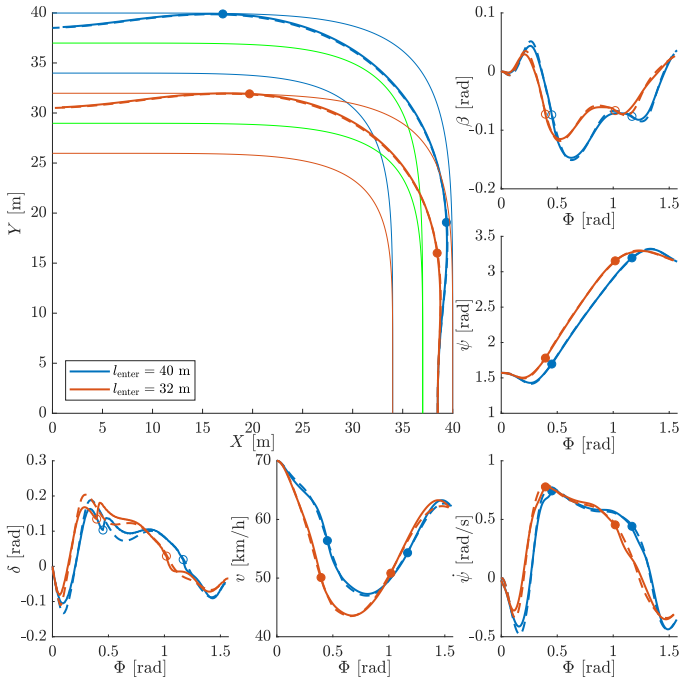


Figure 6: Reconstruction for TM LDP.

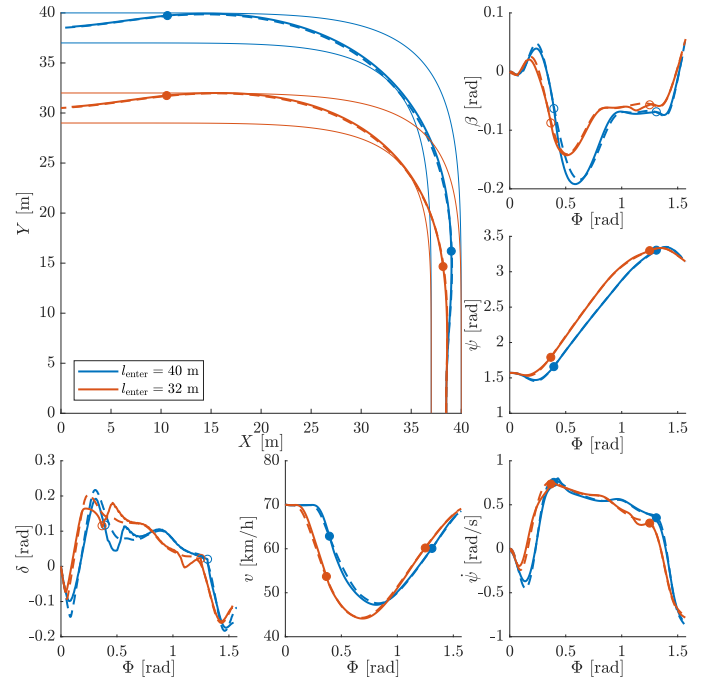


Figure 7: Reconstruction for TM MT.

optimized path after the obstacle, resulting in the increase of the computed objective function in Table 1. This deviation is caused by the use of the simple open-loop simulation strategy with application of the input variables obtained from optimizations without feedback. For the high initial velocity (red lines in Figure 5), the deviation between simulated and optimized path is smaller, which is also reflected in the computed objective function.

The same approach to find segmentation points is evaluated in a minimum-time (MT) optimization objective for DLM (Figure 4). The obtained segmented path and velocity profile (solid lines) are very similar to the optimizations of the full maneuver (dashed lines). Other state variables deviate more for the considered objective function. Splitting points are not uniquely defined at lower velocities, when the vehicle orientation state variable is flat around local extrema.

For the splitting points of the TM, the same reconstruction method is applied. Figures 6 and 7 show path (thick lines) and selected vehicle variables for different entry distances l_{enter} (m). The thin lines show road constraints for the path of the corresponding color. In Figure 6, results are shown for the LDP formulation of the TM. The green lines correspond to the middle of the road (used in the LDP formulation). A small penalty on velocity was added in the objective function for the segmented optimizations to decrease the deviation of the velocity profile for the middle segment. The merged maneuvers are close to the maneuvers obtained from optimizations of the full maneuver.

The method also works for reconstructing trajectories for TM MT, as it is shown in Figure 7. The resulting segmented trajectories are similar to the optimized trajectories. The steering behavior for the middle segment of the segmented maneuver is oscillating more for both objectives, but it does not result in the large deviation of the XY -path.

4.2 Trajectory Computation by Interpolation

In this part, the trajectories are computed for splitting points not present in the database of splitting points, which contains splitting points for a number of maneuvers precomputed offline. Interpolation techniques are used to obtain constraint values of the final states of each segment from the available splitting points in the database. The computed trajectories are compared with optimization results of the full maneuver for the corresponding configuration. It was noticed that the values for the splitting points could be interpolated (see, e.g., the velocity v along the black

line representing the first splitting point in Figure 1, where the velocity values are almost equidistant from each other).

Figures 8–10 show several examples of trajectory computations, where the solid lines show computed trajectories (Comp.), which are obtained by linear interpolation of splitting points (shown in circles) from precomputed trajectories (Used) for maneuvers where some, but not all, parameters of the desired maneuver are matched. The reference trajectory is given by the dash-dotted line (Ref.). The splitting points are obtained by linear interpolation of the splitting points from the used trajectories. Figure 8 illustrates the approach to compute a trajectory for the initial velocity $v_0 = 60$ km/h, using the splitting point values from optimizations of the full maneuver for $v_0 = 50$ km/h and $v_0 = 70$ km/h. The computed maneuver is very similar to the reference maneuver, which is obtained by optimization for the same initial velocity.

The approach was also applied to compute a maneuver for the obstacle width $w = 4$ m using the splitting point values from optimizations of the full maneuver for $w = 3.5$ m and $w = 4.5$ m

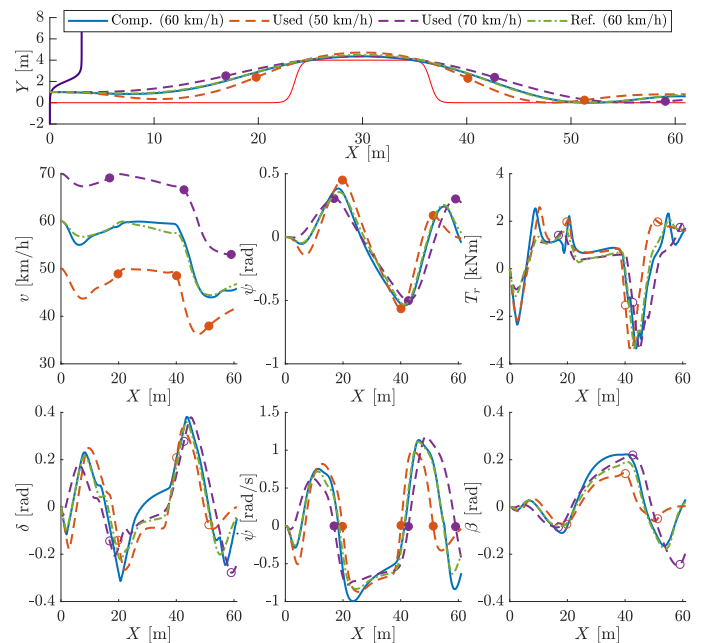


Figure 8: Trajectory computation by interpolation for DLM LDP: initial velocity.

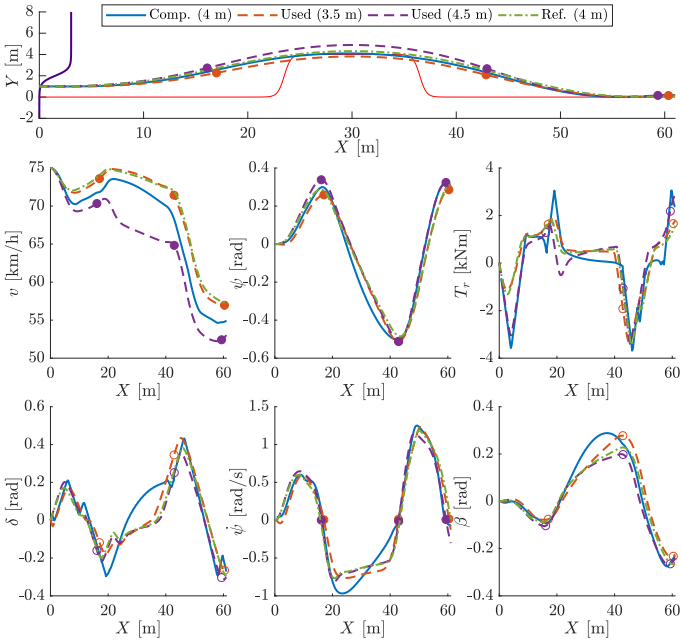


Figure 9: Trajectory computation by interpolation for DLM LDP: obstacle width.

(Figure 9). The computed path is very similar to the reference path, but the velocity profile is slightly different, because a simple algorithm for computing splitting points for the desired maneuver is used. Since the reference velocity profile is very close to one of the used velocity profiles, the assumption about the equidistant distribution of the velocity profiles is not completely valid, causing the obtained velocity profile to be different.

Similar results are obtained for the case of computing a maneuver for an intermediate obstacle length, where splitting points for maneuvers with a shorter and longer obstacle are available in the database. The computed path is very close to the referenced path, but the obtained velocity profile is located in between the used ones, deviating slightly from the reference velocity profile. A remedy for the observed behavior could be a more advanced algorithm for prediction of the values at the splitting points, which affect the computed trajectories.

Figure 10 shows the computed trajectory for LDP in the TM. As it was noted for Figure 2, the state variables for varying entry distances have an appealing distribution resulting in a good match between the computed trajectory for interpolated splitting points and the reference trajectory.

4.3 Constraint Relaxation

For the segmented optimizations, the original constraints together with additional constraints on the final state were used. However, since additional information from the database with splitting points from previous optimizations was used, it was noticed that certain inequality constraints can be relaxed to speed up the optimizations even further.

Figure 11 shows reconstruction results (solid lines) for the same splitting points as in Figure 3, but with obstacle and velocity ($v \leq v_0$) constraints removed from the optimizations. The dashed lines show results obtained when the constraints are present (same results as in Figure 3, which were shown in solid lines before). The removal of the constraints results in slight variations of the state variables, as well as small violations of the XY -path; for the high velocity the vehicle violates the rightmost corner of the obstacle for about 0.07 m along the Y direction.

Some constraints can also be removed for the TM LDP segmented optimizations. The resulting path stays within road boundaries and the state variables have similar behavior compared to the results of the optimization of the full maneuver, with a slight increase in the velocity for the first segment for the longer entry distance.

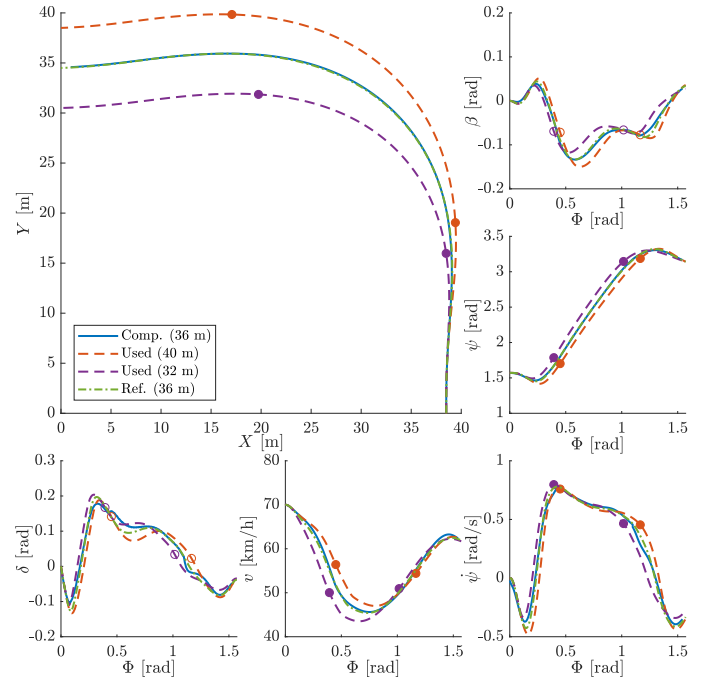


Figure 10: Trajectory computation by interpolation for TM LDP: entry distance.

5 DISCUSSION

The developed splitting–merging technique is based on analysis of optimal trajectories for the full maneuver. A useful method to analyze similarities between trajectories is to illustrate variables for the studied trajectories with an independent variable having the same range for all of them, *e.g.*, the longitudinal variable (X in Figure 1) for the double lane-change maneuver (DLM) or an angle-position variable (Φ in Figure 2) for the 90° -turn maneuver (TM). By taking the length of segments into consideration, such that the length of one segment does not dominate other segments, the final splitting points are selected.

The technique was applied to DLM trajectories obtained by using lane-deviation penalty (LDP) as presented in previous research and to minimum-time (MT) maneuvers. Also, additional variants for TM were obtained for MT and the modified LDP and evaluated using the proposed technique. For the trajectory reconstruction scenario, the segmented trajectories for DLM were similar to the optimized trajectories. The LDP maneuvers have

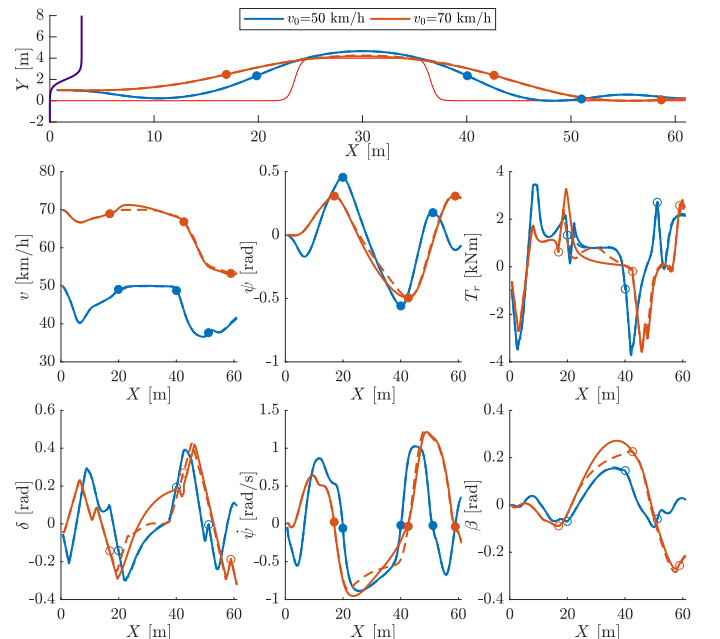


Figure 11: Reconstruction for DLM LDP without the obstacle and velocity constraints. Same splitting points as in Figure 3.

very similar behavior for the vehicle position, orientation, velocity, and body-slip variables, as well as good match for the steering and the front wheel torque input. The MT maneuvers have similar behavior for the vehicle position and velocity. Other variables have a lower match; this is also caused by different behavior of the orientation and yaw rate variables. Splitting points are not uniquely defined when the orientation variable has a flat behavior around the local extrema (Figure 4). The segmentation technique gives best results for maneuvers where the orientation and yaw rate variables have several dominating behaviors in the maneuver.

Segmented trajectories for the TM have a good match to the optimized trajectories for both used objective functions. For this maneuver, the optimization results for MT are similar to the LDP results with a behavior predictable with linear interpolation of the state variables, resulting in good performance of the technique.

For the trajectory computation by interpolation, several cases were considered where available splitting points were differing in one configuration parameter for the problem. The computed trajectories were later compared with the optimization results obtained for the desired configuration parameters. All evaluated parameter variations have a good match for the resulting path. Performance for state variables is naturally dependent on the distribution of the available splitting points. For DLM LDP trajectories with a different initial speed (Figure 8) and TM LDP with a different entry distance (Figure 10) computed by interpolation, the available splitting points were located symmetrically around the desired points, resulting in good prediction of the desired final constraints by linear interpolation, and in a good match of the computed trajectories with the full optimized trajectories. For other computed trajectories (DLM LDP for a different obstacle width and length) the match for the state variables was generally less accurate, *e.g.*, giving lower computed velocity profile for the case with obstacle width (Figure 9). These computed trajectories are still feasible for the considered setup, but exhibit slightly larger values of the objective function.

For the MT formulation, the road constraints were considered for removal and for the LDP formulation, the road constraints together with the velocity constraint were excluded. The resulting segmented trajectories with relaxed constraints are similar to the segmented trajectories with the original constraints (Figure 11). For the DLM LDP path, a small violation of the obstacle was observed. For the TM LDP, the resulting path stayed within road boundaries.

Direct use of the optimized inputs in an open-loop system maybe unfavorable, since simulations showed a mismatch between segmented optimized and simulated trajectories (Table 1, last row, and Figure 5). Combination with a path-following control strategy would be beneficial to use the results from the proposed segmented motion-planning technique. Future research is also to incorporate re-planning capabilities.

6 CONCLUSIONS

To decrease the complexity of computing an optimal vehicle maneuverer, a technique to split a motion-planning optimization problem is developed, which is based on analysis of optimal trajectories for the full maneuver and segmentation based on extrema for the vehicle orientation and the yaw rate. The potential segmentation points are selected by noting similarities between different trajectories, where the values are close to each other or have a favorable distribution for varying parameters of the problem.

Two scenarios were considered: the trajectory reconstruction scenario, when splitting points were available from a database for the same motion-planning configuration, and trajectory computation in an interpolation scenario, where splitting points for similar configurations are available. In each scenario, there was only a small subset of additional final constraints using information from the splitting points imposed, and for most of the

cases, the remaining parts of the problem formulation were left unchanged.

It was successfully investigated to relax certain inequality constraints for the segmented optimizations to decrease the complexity of the problem even further. The resulting segmented trajectories with relaxed constraints are similar to the segmented trajectories with the original constraints.

The proposed technique has shown promising results. It gives close to optimal paths and generally good match for the state variables. The computed segments are feasible and fulfill imposed kinematic and dynamic constraints, with close to the optimal behavior.

ACKNOWLEDGMENT

This work was partially supported by the Wallenberg AI, Autonomous Systems and Software Program (WASP) funded by the Knut and Alice Wallenberg Foundation.

REFERENCES

- [1] J. Ziegler et al. "Making Bertha Drive—An Autonomous Journey on a Historic Route". In: *IEEE Intelligent Transportation Systems Magazine* 6.2 (2014), pp. 8–20.
- [2] A. Arikere, D. Yang, M. Klomp, and M. Lidberg. "Integrated evasive manoeuvre assist for collision mitigation with oncoming vehicles". In: *Vehicle System Dynamics* (2018), pp. 1–27.
- [3] B. Paden, M. Čáp, S. Z. Yong, D. Yershov, and E. Frazzoli. "A survey of motion planning and control techniques for self-driving urban vehicles". In: *IEEE Transactions on Intelligent Vehicles* 1.1 (2016), pp. 33–55.
- [4] P. Falcone, F. Borrelli, J. Asgari, H. E. Tseng, and D. Hrovat. "Predictive Active Steering Control for Autonomous Vehicle Systems". In: *IEEE Transactions on Control Systems Technology* 15.3 (2007), pp. 566–580.
- [5] P. Anistratov, B. Olofsson, and L. Nielsen. "Lane Departure-Based Penalty for Autonomous Avoidance Maneuvers". In: *Accepted for presentation at 14th International Symposium on Advanced Vehicle Control*. Beijing, China, 2018.
- [6] K. Berntorp, B. Olofsson, K. Lundahl, and L. Nielsen. "Models and methodology for optimal trajectory generation in safety-critical road-vehicle manoeuvres". In: *Vehicle System Dynamics* 52.10 (2014), pp. 1304–1332.
- [7] H. Pacejka. *Tyre and vehicle dynamics*. Oxford, UK: Butterworth-Heinemann, 2006.
- [8] Modelica Association. <http://www.modelica.org>. (Date accessed: 30.04.2018).
- [9] J. Åkesson, K.-E. Årzén, M. Gäfvert, T. Bergdahl, and H. Tummescheit. "Modeling and Optimization with Optimica and JModelica.org — Languages and Tools for Solving Large-Scale Dynamic Optimization Problems". In: *Computers and Chemical Engineering* 34.11 (2010), pp. 1737–1749.
- [10] A. Wächter and L. T. Biegler. "On the implementation of an interior-point filter line-search algorithm for large-scale nonlinear programming". In: *Mathematical Programming* 106.1 (2005), pp. 25–57.
- [11] HSL. *A collection of Fortran codes for large scale scientific computation*. <http://www.hsl.rl.ac.uk>. (Date accessed: 30.04.2018).